CVEL

THE CLEMSON UNIVERSITY VEHICULAR ELECTRONICS LABORATORY

TECHNICAL REPORT: CVEL-09-008

IMBALANCE DIFFERENCE MODEL FOR COMMON-MODE RADIATION FROM PRINTED CIRCUIT BOARDS

Changyi Su and Todd Hubing

Clemson University

October 5, 2009

This report was submitted for publication. The revised, peer-reviewed version can be found in the following publication:

C. Su and T. Hubing, "Imbalance difference model for common-mode radiation from printed circuit boards," *IEEE Trans. on Electromagnetic Compatibility*, vol. 53, no. 1, Feb. 2011, pp. 150-156.

EXECUTIVE SUMMARY

The differential-mode signal currents flowing in printed circuit board (PCB) traces are unlikely to produce significant amounts of radiated emissions directly; however these signals may induce common-mode currents on attached cables, enclosures or heatsinks that result in radiated electromagnetic interference. Full-wave EM modeling can be performed in order to determine the level of radiated emissions produced by a PCB trace-board-cable structure, but this modeling is computationally demanding and doesn't provide any physical insight to explain how the differential currents in the signal path became common-mode currents on a distant object.

Various models have been developed to replace the complex PCB trace structure and differential signal currents with an equivalent source that drives the common-mode currents on the PCB structure. Voltage-driven and current-driven common-mode source models, developed at the University of Missouri-Rolla, describe the coupling from differential-mode signals to common-mode currents in terms of the electric and magnetic field coupling, respectively. The imbalance difference model, developed at Okayama University, describe the coupling from differential-mode to common-mode in terms of changes in the imbalance of the differential current carrying structure. Both of these models (voltage/current-driven and imbalance difference) are capable of modeling trace-board structures accurately, yet the equivalent sources derived from them have different amplitudes and locations.

This paper applies the imbalance difference model to trace-board structures and compares the resulting equivalent source configurations to those obtained with the voltage- and current-driven models. It is shown that the imbalance difference model can be factored into two terms that roughly correspond to the voltage-driven and current-driven components. The imbalance difference model has the advantage that is simpler to implement and doesn't require the user to make assumptions regarding the dominant source mechanism. The voltage/current-driven model has the advantage that it can be more intuitive to apply in some situations.

I. INTRODUCTION

Common-mode currents are much more likely to generate significant levels of unintentional radiated emissions than differential-mode currents [1]. For this reason, proper board-level design is required to minimize the common-mode noise currents generated by printed circuit boards (PCBs). Signal traces on PCBs carry differential currents by design, but the signals on these traces can couple to larger nearby objects such as heatsinks, enclosures and attached cables. The common-mode currents induced on these objects can be significant sources of radiated emissions.

For simple PCB structures, the radiated emissions can be calculated using full-wave numerical modeling codes. However, this has approach is limited by the complex models and extensive computational resources required to model the details of each trace structure. In addition, brute-force modeling of the entire board provides relatively little physical insight into the electromagnetic interference (EMI) source mechanisms. Alternatively an effective equivalent model can be obtained by eliminating sources and differential signal structures that do not contribute significantly to the radiated emissions and focusing on the features that could possibly be significant sources of EMI. This equivalent model is generally much simpler than the model-everything full-wave model and it provides good physical insights into the board features that have the greatest impact on radiated emissions. Equivalent models have not only been used to simplify full-wave numerical models, but also to estimate the maximum emissions from PCB structures using closed-form expressions [3]-[5].

Two fundamental mechanisms by which differential-mode sources induce common-mode currents on large structures have been investigated [2]. They are commonly referred to as *current-driven* and *voltage-driven* mechanisms, referring to the prominent differential signal parameter affecting the common-mode currents induced on large external structures. The current-driven mechanism refers to common-mode currents induced by the signal currents returning in the "ground" structure causing voltage differences between objects referenced to different parts of the structure [2, 6, 9]. The voltage-driven mechanism refers to electric-field coupling from traces or heatsinks that are at one potential to cables or other external object that are at a different potential [10]-[12]. An equivalent wire antenna model for estimating voltage-driven common-mode currents was developed in [10]. In this model, the common-mode voltage source is placed at the junction between the ground plane and the attached cable. The magnitude of the equivalent voltage source is expressed in terms of the ratio of the self-capacitances of the board and the trace or heatsink.

These equivalent models are typically applied in situations where it is assumed that one coupling mechanism is dominant. However, for trace-and-board geometries, common-mode currents due to the electric and the magnetic field coupling coexist and can be comparable in strength. Therefore, it is desirable to model the coupling between the differential signals on the board and the common-mode currents on attached cables without specifying a particular field coupling mechanism. In the work presented here, an equivalent model based on the concept of imbalance difference [13] is described. The *imbalance difference model* is another way of describing how differential-mode signals are converted to common-mode voltages and currents based on changes in the degree of imbalance in PCB transmission systems. Using a parameter

called the *current division factor*, the magnitude and location of equivalent common-mode sources can be derived quantitatively. These common-mode sources then replace all of the differential signal structures on the PCB. This paper demonstrates the application of the imbalance difference model to PCB circuit structures and compares the models obtained to current- and voltage-driven models and to full-wave simulations of the entire board structure.

II. DESCRIPTION OF THE IMBALANCE DIFFERENCE MODEL

Fig. 1 schematically shows a typical printed circuit board, where a signal trace is routed over a solid ground plane. The board has cables attached to both ends that are referenced to the ground plane. The microstrip trace is driven at one end and terminated at the other end. The trace-board geometry is electrically small at low frequencies where common-mode currents induced on the cables are likely to be the dominant source of radiated emissions. The space between the trace and the ground plane is filled with a dielectric material with a dielectric constant, ε_r, and a thickness, t. In Fig. 1, the thickness, t, is exaggerated for clarity. In most practical structures, t is several orders of magnitude smaller than L and W.

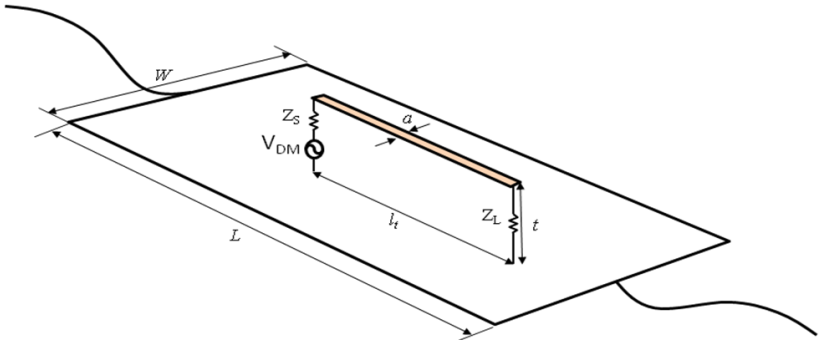

Fig. 1. A trace-board structure with cables attached to the ground plane.

The imbalance difference model was initially proposed to explain the mechanism by which common-mode currents/voltages are induced in PCBs [13] -[17] . A *current division factor* (CDF), which is also referred to as an *imbalance parameter*, can be defined for any transmission line geometry. The imbalance parameter is denoted as "h" in this paper. It is dependent on the cross-sectional structure of the transmission line and therefore changes when two transmission lines of different cross-sectional shapes are connected. The change in the imbalance at the interconnection results in the generation of an equivalent *common-mode voltage source* that can be used to model how common-mode currents are induced on the structure. Using Fig. 2 as an example, there is a change in the imbalance parameter, h, at both ends of the microstrip. At each end, the width of the trace varies from a finite value, a, to zero. At the discontinuity points A and B, as shown in Fig. 2 (a), common-mode voltages are generated in the ground plane and their magnitudes are computed as the product of the differential-mode voltage and the change in the imbalance parameter [13] ,

$$\Delta V_C(x) = \Delta h V_N(x), \tag{1}$$

Where V_N is the differential-mode voltage between the signal trace and the return plane, and x denotes the location of the common-mode excitation. According to (1), the common-mode excitation at location A is computed by,

$$\Delta V_C(A) = (h_2 - h_1) V_N(A), \tag{2}$$

and the common-mode excitation at B is

$$\Delta V_C(B) = (h_3 - h_2) V_N(B). \tag{3}$$

The common-mode equivalent circuit is excited by $\Delta V_C(A)$ and $\Delta V_C(B)$, which are placed on the board at points A and B, respectively, as shown in Fig. 2(b).

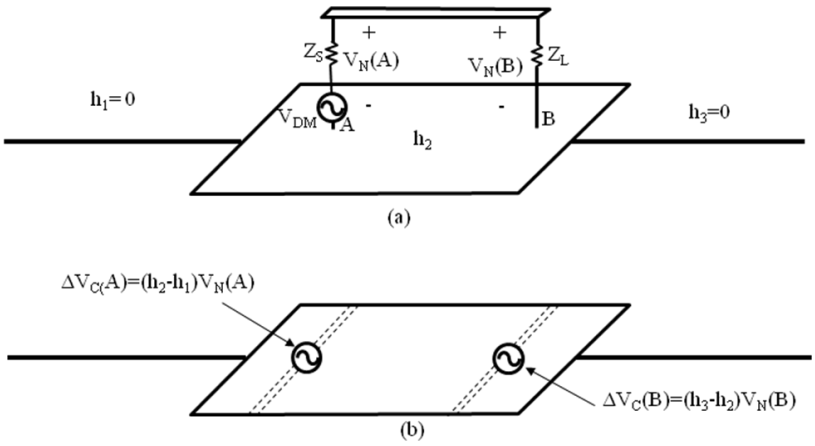

Fig. 2. Imbalance difference model: (a) trace-and-board configuration (b) equivalent model.

As indicated in (2) and (3), the relationship between the differential-mode and common-mode source amplitudes is completely determined by the change of the imbalance parameter. The imbalance parameter, h, is defined as,

$$h = \frac{I_{CM-return}}{I_{CM}}, \tag{4}$$

where I_{CM} and $I_{CM\text{-}return}$ are the total common-mode current and the common-mode current flowing on the signal trace, respectively [16] . For microstrip trace structures, this parameter is given by [14]

$$h = \frac{L_{return}}{L_{return} + L_{trace}}, \tag{5}$$

where L_{return} and L_{trace} are the partial inductances of the ground and the signal trace, respectively. The imbalance parameter for the portions of the structure extending beyond the trace is zero. The

imbalance parameter for the trace-board portion, h_2, must always be between zero and one. Since h_1 and h_3 are zero and the common-mode voltages in (2) and (3) can be rewritten as,

$$V_{CM}(A) = h_2 V_N(A), \tag{6}$$

and

$$V_{CM}(B) = -h_2 V_N(B). \tag{7}$$

III. IMBALANCE DIFFERENCE COMPARED TO VOLTAGE- AND CURRENT-DRIVEN MODELS

A. Imbalance difference model for the trace-board configuration

Fig. 3 illustrates the imbalance difference model for the trace-board configuration of Fig. 1 after the trace and differential-mode source have been replaced by the equivalent common-mode sources. Expressed as a function of the trace current, the magnitude of the differential-mode voltage between the trace and the ground plane at point A in Fig. 1 is,

$$V_N(A) = \left| j2\pi f \left(L_{return} + L_{trace} \right) I_{DM} + Z_L I_{DM} \right|. \tag{8}$$

Combining (5), (6) and (8), the equivalent common-mode voltage at point A is,

$$V_1 = \left| j2\pi f L_{return} I_{DM} + \frac{L_{return}}{L_{trace} + L_{return}} Z_L I_{DM} \right|, \tag{9}$$

where I_{DM} is the differential-mode current. Taking the differential-mode current as a reference, the phasor expression for the common-mode voltage is

$$\begin{aligned} \mathbf{V_1} &= 2\pi f L_{return} I_{DM} \angle 90^\circ + \frac{L_{return}}{L_{trace} + L_{return}} Z_L I_{DM} \angle 0^\circ \\ &\approx 2\pi f L_{return} I_{DM} \angle 90^\circ + \frac{L_{return}}{L_{trace} + L_{return}} \frac{Z_L}{Z_S + Z_L} V_{DM} \angle 0^\circ \end{aligned}. \tag{10}$$

Similarly, the equivalent common-mode voltage at point B is given by

$$V_2 = \frac{L_{return}}{L_{trace} + L_{return}} \frac{Z_L}{Z_S + Z_L} V_{DM}. \tag{11}$$

Fig. 3. Imbalance difference model for the trace-board configuration in Fig. 1.

The value of the plane's partial inductance is related to the geometry and location of the trace relative to the return plane. Starting from an analytical result using conformal mapping, an expression for the partial inductance of the return plane is given by [9]:

$$L_{return} = \frac{\mu_0}{\pi}\frac{tl_t}{W}\frac{1}{\sqrt{1-4\left(1-2t/W\right)\left(s/W\right)^2}}, \tag{12}$$

where s is the offset of the trace from the center of the board. The above closed-form expression was derived by assuming the separation, t, and the trace width, a, are much smaller than $W/2$. The dielectric constant is neglected in the derivation, which is a valid simplification for the quasi-static limits of the magnetic field.

From (10) and (11), the equivalent model consists of two parts. One part is the first term in (10), which is proportional to the differential-mode current. The other part is the second term in (10) and (11), which is proportional to the differential-mode voltage. It is interesting to compare the imbalance difference model to a combination of Hockanson's current-driven model [6] and Shim's voltage-driven model [10] as shown in Fig. 4. In Hockanson's model, one equivalent voltage source is placed at the midpoint of the current return path on the board. The magnitude of the source is proportional to the differential-mode current flowing through the trace,

$$V_1 = 2\pi f L_{return} I_{DM}\,. \tag{13}$$

In Shim's voltage-driven model, equivalent voltage sources are placed at the junctions between the cables and the plane. The magnitudes of the voltage sources are expressed in terms of the ratio of the self-capacitances of the board and the trace,

$$V_2 = V_3 = \frac{C_{trace}}{C_{board}}\frac{Z_L}{Z_S + Z_L}V_{DM}\,. \tag{14}$$

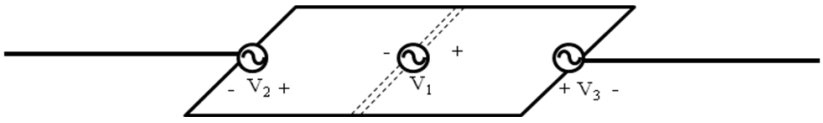

Fig. 4. Equivalent model based on Hockanson's and Shim's models.

Although the two equivalent models (Figs. 3 and 4) differ in the number, the locations, and the magnitudes of the equivalent sources, they are both equivalent to the original trace-board configuration. It is demonstrated in the next section that the predicted radiated emissions using the two models agree well at frequencies up to 500 MHz.

B. Equivalent models for shorted and open trace configurations

A shorted-trace configuration is a special case of Fig. 2(a) that enhances the current-driven coupling and suppresses the voltage-driven coupling to the cables. Hence, this configuration, as

shown in Fig. 5(a), is used to demonstrate the current-driven source mechanism. At point A, the equivalent common-mode voltage is given by (2),

$$\begin{aligned} V_{CM} &= h_2 V_N(A) \\ &= \frac{L_{return}}{L_{return}+L_{trace}} 2\pi f \left(L_{return}+L_{trace}\right) I_{DM} . \\ &= 2\pi f L_{return} I_{DM} \end{aligned} \tag{15}$$

The loop inductance causes the differential current I_{DM} to lag the differential-mode voltage V_{DM}. Assuming the phasor of the differential current is $I_{DM}\angle 0^\circ$, the common-mode voltage in (15) can be expressed using phasor notation as,

$$\mathbf{V_{CM}} = 2\pi f L_{return} I_{DM} \angle 90^\circ . \tag{16}$$

The trace is shorted to the ground plane at the load side; so according to (3), the magnitude of the equivalent common-mode excitation at point B is zero,

$$\Delta V_C(B) = -h_2 V_N(B) = 0 . \tag{17}$$

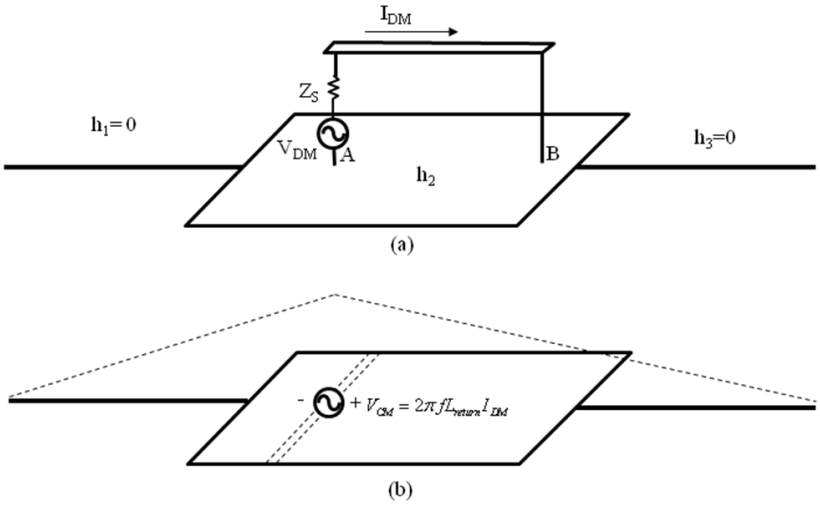

Fig. 5. Imbalance difference model for the shorted trace structure.

Note that the magnitude of the common-mode source in the imbalance difference model, (16), is identical to (13), which was obtained [6] using a different approach. However, in the two models, the common-mode voltage source is placed on the board at different locations. In the imbalance difference model shown in Fig. 5(b), the common-mode source is placed on the board at the feed point of the trace. In the current-driven model, the common-mode source is located at the center point of the current return path on the board.

To enhance the voltage-driven coupling and suppress the current-driven coupling to the cables, the load end of the trace is open-circuited as shown in Fig. 6(a). Since the imbalance parameter is independent of the loading condition, (5) is still valid for the open-circuit case. Therefore, the magnitude of the equivalent common-mode voltage is,

$$V_{CM} = \frac{L_{return}}{L_{return} + L_{trace}} V_{DM} \,. \tag{18}$$

Two common-mode voltage sources are placed on the return plane with the same magnitudes but opposite phases. Using conformal mapping, the self-inductance of the trace over a finite ground plane is given by [18] ,

$$L_{trace} = \begin{cases} \dfrac{\mu_0 l_t}{2\pi} \ln\left(\dfrac{8t}{a} + \dfrac{a}{4t}\right) & \dfrac{a}{t} \le 1 \\ \mu_0 l_t \left[\dfrac{a}{t} + 1.393 + 0.667 \ln\left(\dfrac{a}{t} + 1.444\right)\right]^{-1} & \dfrac{a}{t} \ge 1 \end{cases} . \tag{19}$$

The equivalent antenna model for the voltage-driven mechanism is shown in Fig. 6(b).

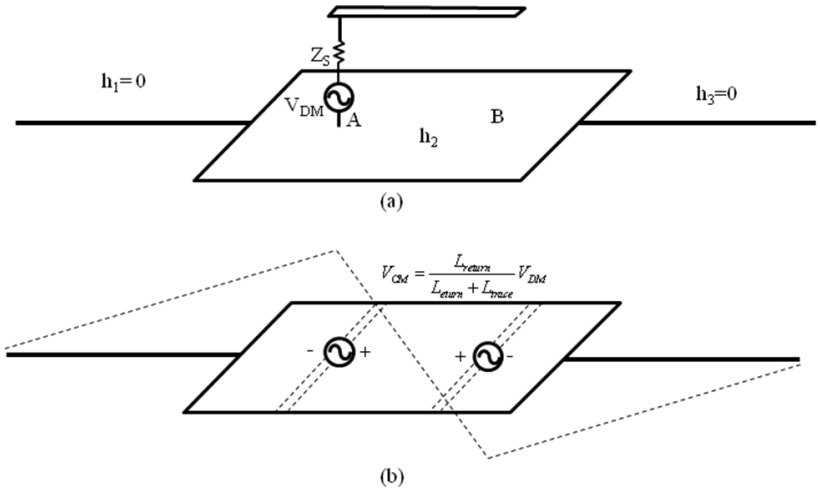

Fig. 6. Imbalance difference model for the open trace structure.

The dashed line in Fig. 6(b) represents the common-mode current distribution over the configuration. The current is nearly symmetric about the center of the board if the maximum dimension of the board is much smaller than that of the cables. In the equivalent model of the voltage-driven mechanism in Fig. 6(b), two common-mode voltage sources are placed at point A and B, respectively. They have the same magnitude but opposite phases. Hence, the common-mode current distribution is mirrored across the center of the board. It is noted that the current-driven mechanism induces common-mode currents that flow in the same direction on the two cables, while

the voltage-driven mechanism induces common-mode currents that flow in opposite directions on the two cables. Therefore, when both mechanisms are significant, the total common-mode current will not be the same on both wires.

IV. MODELING EXAMPLES

A. Trace terminated with 50 ohms

To evaluate the imbalance difference models described in the previous section, numerical simulations of the trace-board configuration in Fig. 1 were performed. The maximum radiated electric fields at a distance of 3 meters were calculated for both the original configuration (modeling the entire trace-board structure) and the equivalent common-mode models (i.e., the imbalance difference model, current-driven model and voltage-driven model). The simulations were performed using a full-wave electromagnetic modeling code (FEKO) [19] based on the method of moments.

The board dimensions were 10 cm x W cm, where W is the width of the board. A 5-cm long, 1-mm wide trace was placed 3 mm above the board, and two 50-cm cables were attached to the board and oriented horizontally. A 2-V source with a50-ohm series impedance was connected between one end of the trace and the ground plane. The other end of the trace was terminated by a 50-ohm resistor. The board was located in free space.

Fig. 7 shows the maximum radiated electric fields obtained from 4-cm and 10-cm wide boards. The red solid curve is the maximum radiation obtained from a full-wave model of the entire configuration. As indicated by (5) and (12), the imbalance parameter can be reduced by widening the ground plane. Hence, the common-mode radiated emissions from the 10-cm wide board are about 8 dB lower than the emissions from the 4-cm wide board. This observation is consistent with the experimental results in [6].

In Figure 7, the green dashed line and blue dash-dot line represent the results obtained from the imbalance difference model in Figure 3 and the Hockanson-Shim model in Figure 4, respectively. Both equivalent models agree well with the original configuration, particularly near the resonant peaks.

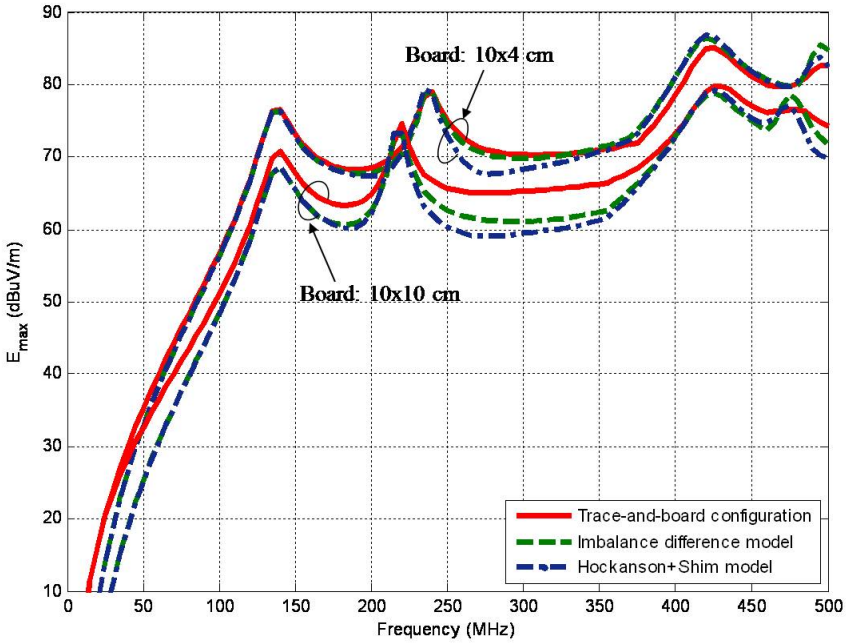

Fig. 7. Comparison of the radiated emissions from the full trace-board configuration and the two equivalent models.

B. Trace terminated with 0 ohms

The imbalance difference model replaces the current-driven and voltage-driven common-mode EMI source models, eliminating the need to make assumptions about which source model is dominant in a given situation. To illustrate the value of this, the geometry in the previous section was modelled with the trace shorted to the ground plane at the load. The source amplitude was 2 V and the source impedance was 100 ohms. This is a configuration where the current-driven mechanism is expected to dominate. The current is approximately the same as it was in the 50-ohm load configuration, but the voltage is significantly reduced.

The maximum 3-meter radiation from 4-cm and 10-cm wide boards was calculated using the imbalance difference model and compared to results obtained by analyzing the original trace-board configuration. The emissions from the shorted-trace configuration are shown in Figure 8(a). The solid line is the result obtained from analysis of the complete trace-board structure. The dashed line represents the simulation result for the imbalance difference model. The magnitude of the equivalent common-mode voltage was computed using (15). Figure 8(b) compares the maximum electric field radiated from the open-circuited board using both the original model and the

imbalance difference model. In this case, the magnitudes of the equivalent common-mode excitations were computed using (18).

As discussed in the previous section, the current-driven model employs one equivalent common-mode voltage source that, for the shorted-trace configuration, has the same magnitude as the imbalance difference model. However, while the common-mode source is generally placed at the midpoint of the current return path in the current-driven model, the imbalance difference model places the source in the return path where the source end of the trace was.

The simulation results in Figure 9 show that both models calculate the maximum radiation from the shorted-trace configurations with reasonable accuracy. However, the current-driven model fails to predict the small peaks at 235 MHz and 215 MHz for 10×4 cm and 10×10 cm boards, respectively. Further analysis shows that these peaks are caused by the voltage difference between the trace and the ground plane, which is zero at the load, but non-zero away from the load due to the inductance of the trace. Although the current-driven peaks are dominant, the voltage-driven mechanism cannot be neglected, even with a shorted trace.

The imbalance difference model calculated both the current- and voltage-driven components as shown in Figure 9. Similarly, the imbalance difference model successfully predicts the peaks at 495 MHz (the second resonance of the 10 x 4 cm board being driven relative to the cables) and 475 MHz (the second resonance of the 10 x 10 cm board being driven relative to the cables). These two peaks don't show up in the current-driven model results.

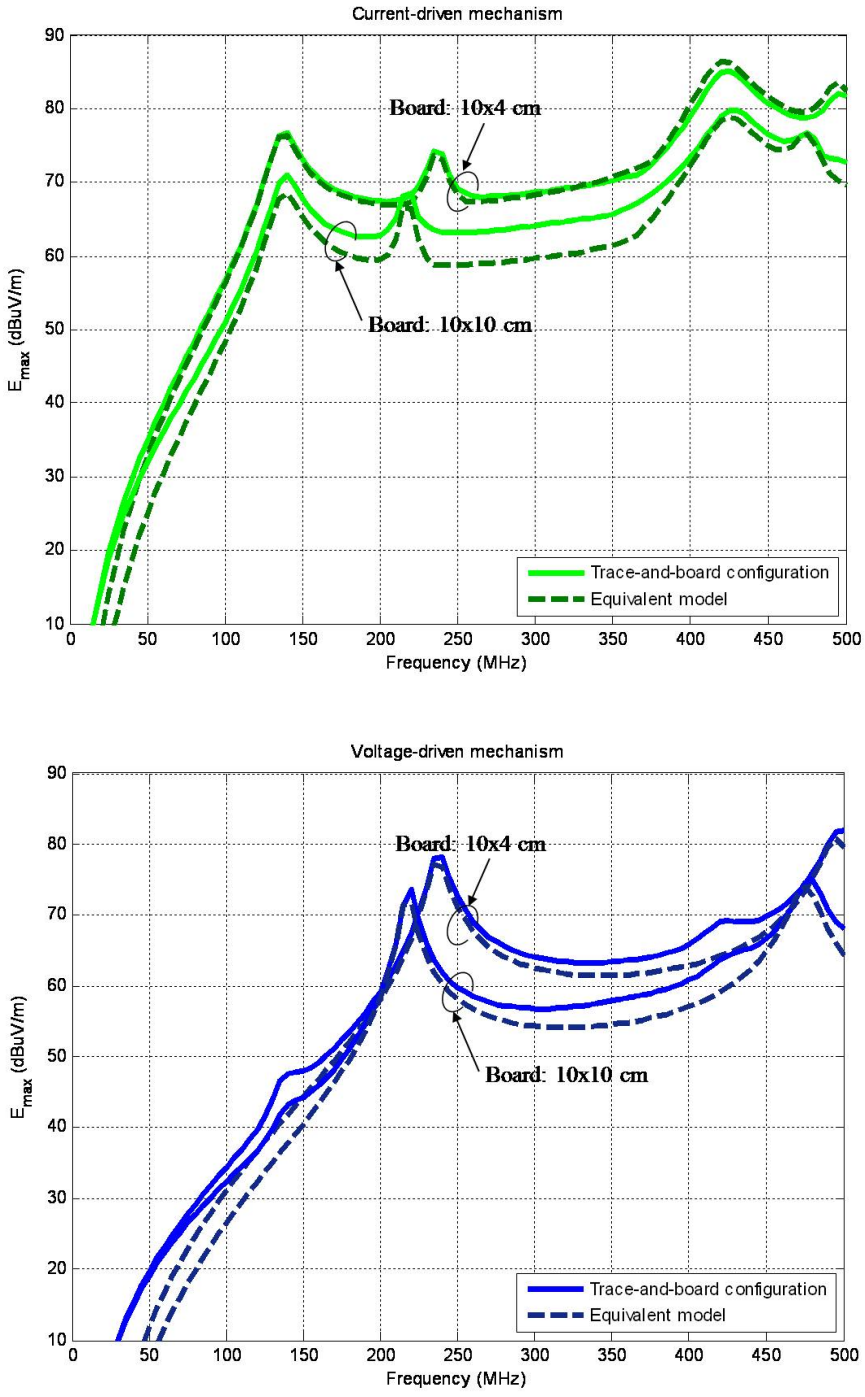

Fig. 8. Comparison of the radiated emissions calculated using the trace-board configuration and the imbalance difference model from shorted trace (upper plot) and open trace (lower plot).

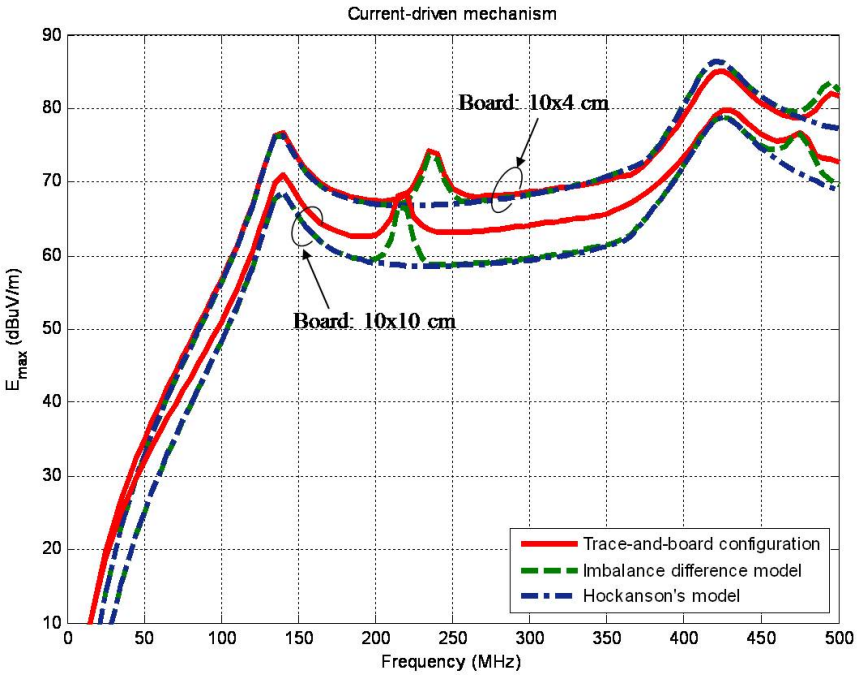

Fig. 9. Comparison of the radiated emissions from the shorted-trace configuration calculated from the imbalance difference model and current-driven model.

C. Trace located near the board edge

It has been demonstrated experimentally and through numerical modeling that the radiated fields increase as a trace is brought in proximity to the board edge. Berg *et. al*. [20] explained that the increment in the radiated emissions is the result of increased magnetic flux beneath the board. Explained in terms of the imbalance difference model described in Section III, the imbalance parameter of the trace-board pair increases as the trace is moved towards the board edge.

To verify this, boards were evaluated with different trace positions. Figure 10 shows a 10 cm x 10 cm board with a cable attached to each side. A 1-mm wide trace is 5 cm long and 1 mm above the ground plane. Two different positions of the trace were considered. The maximum radiated fields from the board are shown in Fig. 11. The simulation results show that the radiated field is stronger as the trace is brought in proximity to the board edge. The imbalance parameter is 0.0185 for the trace at position 1 and 0.029 for the trace at position 2; resulting in a 5 dB [$\approx 20\log_{10}(0.029/0.0185)$] difference at 220 MHz. The imbalance difference model results agree well with the trace-board configuration results over the entire frequency range evaluated.

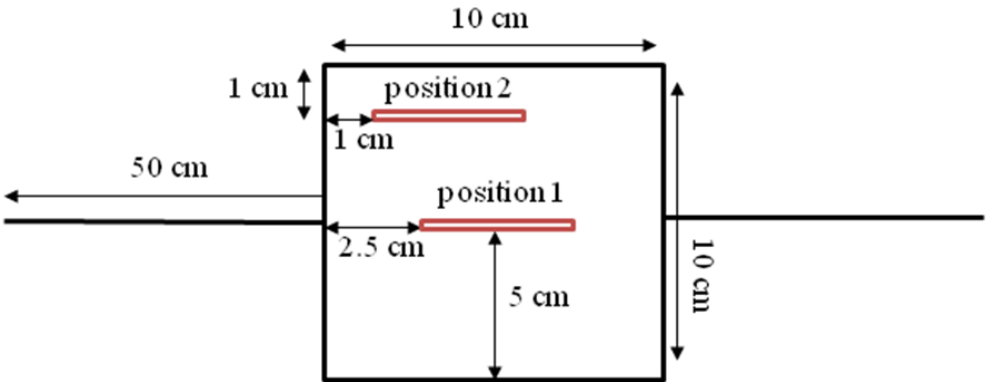

Fig. 10. Test board configuration with different trace positions.

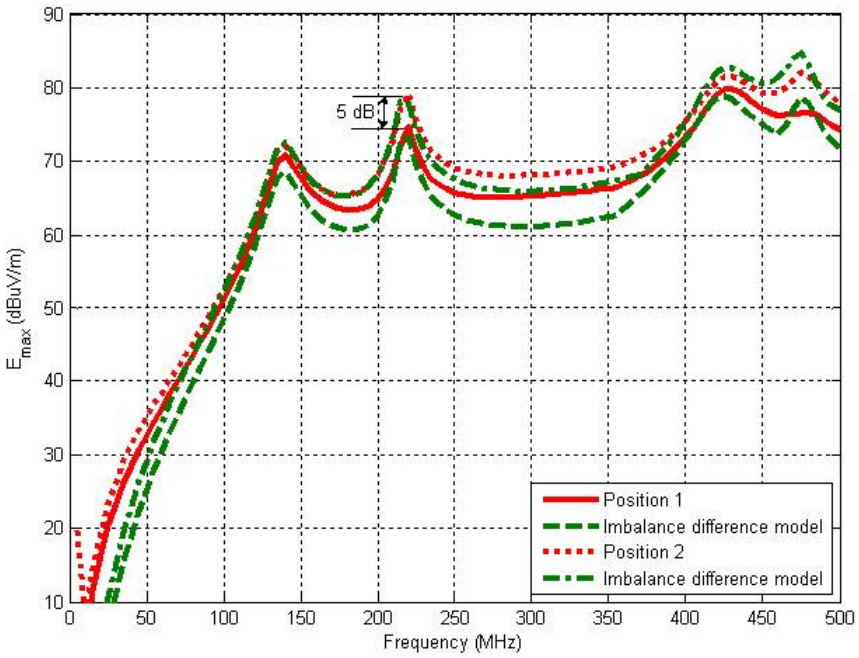

Fig. 11. Comparison of radiated fields from the trace-board configuration and the imbalance difference model for two trace positions.

V. CONCLUSIONS

The imbalance difference model was used to estimate the radiated emissions from trace-board structures due to common-mode currents induced on attached cables. The results obtained were compared to results obtained with voltage/current-driven models. Both models produced accurate results even though they employed equivalent sources that had different amplitudes and locations. The imbalance difference model has the advantage that is simpler to implement and doesn't require the user to make assumptions regarding the dominant source mechanism. The voltage/current-driven model has the advantage that it can be more intuitive to apply in some situations.

REFERENCES

[1] C. R. Paul, *Introduction to Electromagnetic Compatibility*, John Wiley & Sons, New York, 1992.

[2] J. L. Drewniak, T. H. Hubing, and T. P. Van Doren, "Investigation of fundamental mechanisms of common-mode radiation from printed circuit boards with attached cables," in *Proc. IEEE Int. Symp. Electromagnetic Compatibility*, Chicago, IL, Aug. 1994, pp. 110-115.

[3] H. Shim, T. Hubing, T. P. Van Doren, R. DuBroff, J. Drewniak, D. Pommerenke, R. Kaires, " Expert system algorithms for identifying radiated emission problems in printed circuit boards," in *Proc. IEEE int. Symp. Electromagnetic Compatibility*, Santa Clara, CA, Aug. 2004, pp. 57-62.

[4] Navin Kashyap, *An Expert System Application in Electromagnetic Compatibility*, M. S. Thesis, University of Missouri-Rolla, 1997.

[5] Y. Fu and T. Hubing, "Analysis of radiated emissions from a printed circuit board using expert system algorithms," *IEEE Trans. Electromagn. Compat.*, vol. 49, no. 1, pp. 68-75, Feb. 2007.

[6] D. M. Hockanson, J. L. Drewniak, T. H. Hubing, T. P. Van Doren, F. Sha, and M. Wilhelm, "Investigation of fundamental EMI source mechanisms driving common-mode radiation from printed circuit boards with attached cables," *IEEE Trans. Electromagn. Compat.*, vol. EMC-38, no. 4, pp. 557-566, Nov. 1996.

[7] D. M. Hockanson, J. L. Drewniak, T. H. Hubing, T. P. Van Doren, F. Sha, C. W. Lam, and L. Rubin, "Quantifying EMI resulting from finite-impedance reference planes," *IEEE Trans. Electromagn. Compat.*, vol. EMC-39, no. 4, pp. 286-297, Nov. 1997.

[8] G. Dash, J. Curtis, and I. Straus, "The current-driven model-experimental verification and the contribution of I_{dd} delta to digital device radiation," in *Proc. IEEE Int. Symp. Electromagnetic Compatibility*, Seattle, WA, Aug. 1999, pp. 317-322.

[9] M. Leone, "Design expressions for trace-to-edge common-mode inductee of a printed circuit board," *IEEE Trans. Electromagn. Compat.*, vol. 43, no. 4, pp. 667-671, Nov. 2001.

[10] H. Shim and T. Hubing, "Model for estimating radiated emissions from a printed circuit Board with attached cables driven by voltage-driven sources," *IEEE Trans. Electromagn. Compat*., vol. 47, no. 4, pp. 899-907, Nov. 2005.

[11] H. Shim and T. Hubing, "Derivation of a closed-form expression for the self-capacitance of a printed circuit board trace*," IEEE Trans. Electromagn. Compat.*, vol. 47, no. 4, pp. 1004-1008, Nov. 2005.

[12] S. Deng, T. Hubing and D. Beetner, "Estimating maximum radiated emissions from printed circuit boards with an attached cable," *IEEE Trans. Electromagn. Compat*., vol. 50, no. 1, pp. 215-218, Feb. 2008.

[13] T. Watanabe, O, Wada, Y. Toyota, and R. Koga, "Estimation of Common-mode EMI Caused by a Signal Line in the Vicinity of Ground Edge on a PCB," in *Proc. IEEE Int. Symp. Electromagnetic Compatibility*, Minneapolis, Aug. 2002, pp.113-118.

[14] T. Watanabe, et al., "Equivalence of two calculation methods for common-mode excitation on a printed circuit board with narrow ground plane," in *Proc. IEEE Int. Symp. Electromagnetic Compatibility*, Boston, MA, Aug. 2003, pp. 22-27.

[15] O. Wada, "Modeling and simulation of unintended electromagnetic emission from digital circuits," IEICE Transactions on Communications (Japanese Edition), vol. 87, no. 8, pp. 1062-1069, July 2003.

[16] Y. Toyota, et al., "Prediction of electromagnetic emissions from PCBs with interconnections through common-mode antenna model," in *Proc. IEEE Int. Symp. Electromagnetic Compatibility*, Zurich, Sept. 2007, pp. 107-110.

[17] Y. Toyota, T. Matsushima, K. Iokibe, R. Koga, T. Watanabe, "Experimental validation of imbalance difference model to estimate common-mode excitation in PCBs," in *Proc. IEEE Int. Symp. Electromagnetic Compatibility*, Detroit, Aug. 2008, pp. 1-6.

[18] D. M. Pozar, *Microwave Engineering*, MA: Addison-Wesley, 1990.

[19] *FEKO User's Manual,* Suite 5.5, July 2009.

[20] D. Berg, M. Tanaka, Y. Ji, X. Ye, J. Drewniak, T. Hubing, R. DuBroff, and T. Van Doren, "FDTD and FEM/MOM modeling of EMI resulting from a trace near a PCB edge," *Proc. IEEE Int. Symp. Electromagnetic Compatibility,* Washington, D.C., Aug. 2000, pp. 135-140.